SIRIUS STORAGE RING RF PLANT IDENTIFICATION

D. Daminelli*, F. K. G. Hoshino, A. P. B. Lima,

Brazilian Synchrotron Light Laboratory, Campinas, Brazil

M. Souza, University of Campinas, Campinas, Brazil

Abstract

The design configuration of the Sirius Light Source RF System is based on two superconducting RF cavities and eight 65 kW solid-state amplifiers operating at 500 MHz. The current configuration, based on a 7-cell normal conducting PETRA cavity, was initially planned for commissioning and initial tests of the beamlines. A digital low-level RF (DLLRF) system based on ALBA topology has been operating since 2019. Sirius is currently operating in decay mode for beamline tests with 100 mA stored current. During the commissioning, several studies were carried out to increase the stored current with stable beam. This paper presents a study using parametric data-driven models to identify the Storage Ring RF plant, aiming to optimize the DLLRF PI control parameters.

INTRODUCTION

Sirius's current Storage Ring RF system is operating with a 7-cell normal conducting cavity driven by a 130 kW RF Plant consisted of two 65 kW solid state amplifiers (SSA). THe RF System is controlled by a digital low-level RF (DLLRF) [1] based on the ALBA's design to achieve 0.1 % amplitude and 0.1 ° phase stability under normal operating conditions [2, 3].

Until now, the DLLRF controller parameters were tuned with a pragmatic approach to ensure beam stability. In order to optimize these parameters, improving output disturbance rejection, and mitigate longitudinal instabilities [4], a study has been conducted to identify the RF plant and find a parametric polynomial model that can be used along with MATLAB's Control Toolbox [5] to fine tune the PI loop. The methods and results of this study are discussed in the following sections.

RF PLANT STRUCTURE

Figure 1 shows a block diagram from the Sirius Storage Ring RF System.
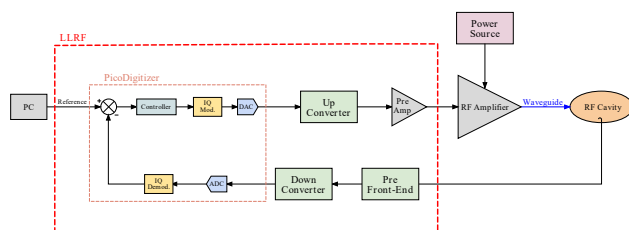
Figure 1: Sirius RF Plant block diagram.

---

* david.daminelli@cnpem.br

The PicoDigitizer from Nutaq [6] houses the Virtex-6 SX315T FPGA and two FMC boards: a 16-channel 14-bit 125 MSPS ADC board and a 8-channel 16-bit 250 MSPS DAC board.

Regarding the many features available in LLRF, some were particularly useful for this study:

- IQ Digital Modulation/Demodulation
- PI Loops for Cavity Voltage Control in IQ (rectangular) or Polar loops
- Phase Shifters and Gain control on each DAC's outpus and ADC's Input
- Fast Data Logger (FDL) for fast data acquisition and post-mortem analysis
- Conditioning mode with a 10 Hz square-modulated RF Drive output.

LINEAR MODEL

System modelling and identification are very useful tools to extract information about a system from measured input-output data and to aid the design of high-performance controllers [7]. There are multiple ways of representing a system, but some are especially suitable for system identification, as they are based on well-established algorithms [8].

Parametric Polynomial Models

In this study, linear discrete representations fits well for this application. A general discrete model can be written as follows:

$$y(k) = \frac{B(q)}{A(q)F(q)}u(k) + \frac{C(q)}{A(q)D(q)}v(k), \qquad (1)$$

with q being the delay operator, that is $y(k)q^{-1} = y(k-1)$, $v(k)$ a white Gaussian noise and $A(q)$, $B(q)$, $C(q)$, $D(q)$, and $F(q)$ the following polynomials:

$$A(q) = 1 - a_1 q^{-1} - \cdots - a_{n_y} q^{-n_y}$$
$$B(q) = b_1 q^{-1} + \cdots + b_{n_u} q^{-n_u}$$
$$C(q) = 1 + c_1 q^{-1} + \cdots + c_{n_v} q^{-n_v} \qquad (2)$$
$$D(q) = 1 + d_1 q^{-1} + \cdots + d_{n_d} q^{-n_d}$$
$$F(q) = 1 + f_1 q^{-1} + \cdots + f_{f_v} q^{-f_v}.$$

From the generic model shown in (1) we can obtain simpler models useful for the identification of several types of systems. For this study, an Output Error model, shown in Eq. (3) was chosen to describe the RF Plant.

$$y(k) = \frac{B(q)}{F(q)}u(k) + v(k) \qquad (3)$$

MC6: Beam Instrumentation, Controls, Feedback and Operational Aspects

T27: Low Level RF

IQ Demodulation

Sirius's DLLRF is based on an IQ modulation/demodulation technique. A signal $x(t)$ centered on a carrier at ω_c rad/s can be expressed as following:

$$x(t) = x_i(t)cos(\omega_c t) - x_q(t)sin(\omega_c t), \qquad (4)$$

where $x_i(t)$ and $x_q(t)$ are, respectively, the In-Phase and Quadrature base-band envelopes.

The transmission of $x(t)$ over a system with impulse response $h(t)$ can be obtained from the convolution product:

$$y(t) = h(t) * x(t). \qquad (5)$$

From Eq. (4) and (5), analysing in base-band, we derive that [9]:

$$\begin{bmatrix} y_i(t) \\ y_q(t) \end{bmatrix} = \begin{bmatrix} h_s(t) & h_c(t) \\ -h_c(t) & h_s(t) \end{bmatrix} * \begin{bmatrix} x_i(t) \\ x_q(t) \end{bmatrix}, \qquad (6)$$
$$h_s(t) = h_{ii}(t) = h_{qq}(t) = h(t)cos(\omega_c t),$$
$$h_c(t) = h_{qi}(t) = -h_{iq}(t) = -h(t)sin(\omega_c t),$$

where $y_i(t)$ and $y_q(t)$ are, respectively, the output In-Phase and Quadrature base-band envelopes.

Therefore, two linear models must be found when modeling the system: one for the straight impulse response $h_s(t)$ and one for the crossed impulse response $h_c(t)$.

DATA PROCESSING

Using the FDL and Conditioning Mode, a set of data was collected from the RF plant in open loop. As previously demonstrated in Eq. (6), two sets of transfer functions must be modeled: a straight one, which can be obtained by driving the I input and measuring the I output (same for Q input and output), and a crossed one, which can be obtained by driving the I input and measuring the Q output (same for Q input and I output). The data obtained by driving the I input only can be seen in Fig. 2a, linearized around the operating point. The output was measured in the cavity, acquired by the LLRF. Similar data was obtained by driving Q only, in addition to other amplitude values.

The IQ data collected is digitized by the PicoDigitizer at a 41.6 MHz sample rate. Despite the large frequency resolution, the LLRF can only perform in a bandwidth of a few tens of kHz. Therefore, the data can be filtered and decimated without loosing useful information, thus reducing the noise and the identification algorithms runtime.

Furthermore, an oscillation around 60 Hz is noticeable. A notch filter was applied to mitigate this noise.

Figure 2b shows the data after the processing described previously.

RESULTS

MATLAB's System Identification Toolbox [10] were used to estimate the functions and compare with validation data. This comparison can be seen in Fig. 3.

(a) Raw data

(b) Processed data
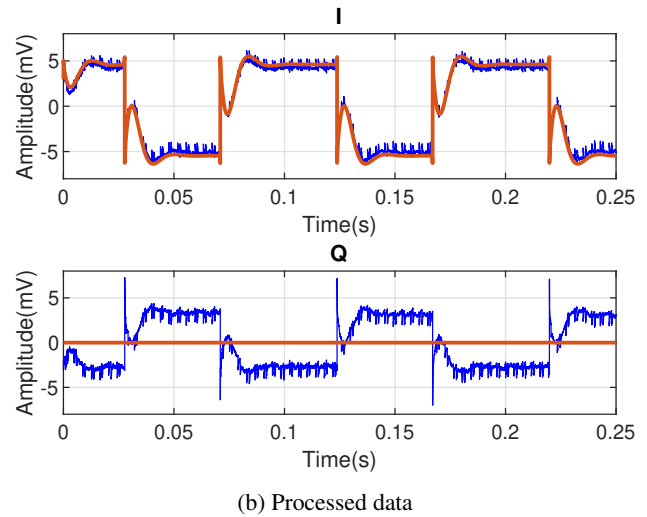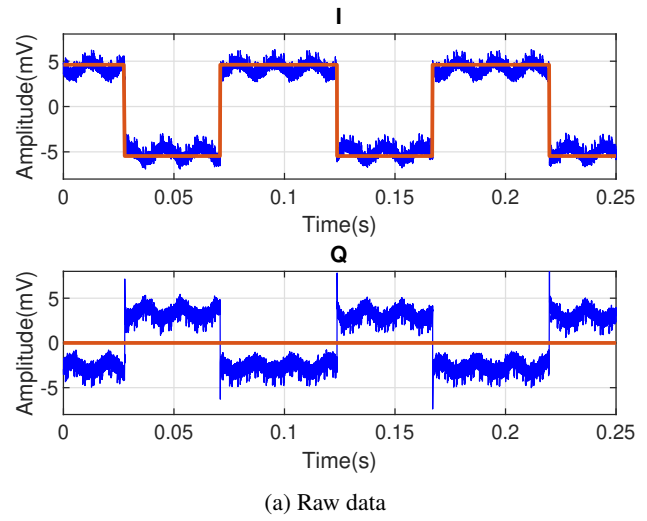
Figure 2: I and Q output (blue) signals obtained by driving I input only (orange).
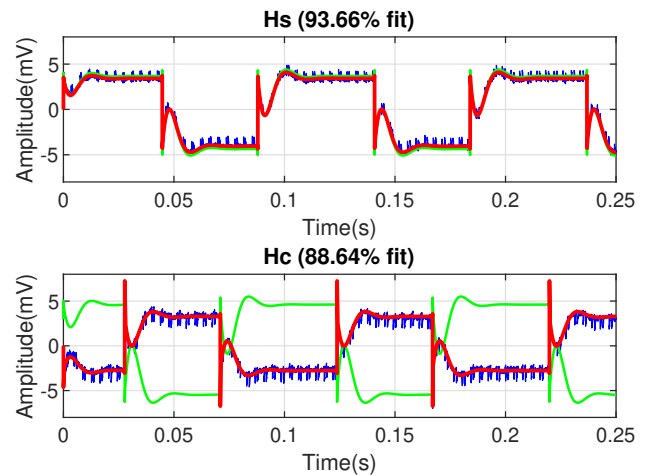
Figure 3: Estimated models outputs (red) compared to measured validation data (blue) when driven by the same input signal (green).

Equations (7) and (8) present, respectively, the estimated straight (H_s) and crossed (H_c) transfer functions.

$$H_s = \frac{0.0315z^{-1} - 0.02851z^{-2}}{1 - 3.228z^{-1} + 4.068z^{-2} - 2.391z^{-3} + 0.5548z^{-4}} \tag{7}$$

$$H_c = \frac{0.07778z^{-1} - 0.07649z^{-2}}{1 - 2.197z^{-1} + 1.238z^{-2} + 0.1991z^{-3} - 0.2381z^{-4}} \tag{8}$$

A way to validate the complete model is by applying a linear combination of the measured data on its input. To do so, the block diagram shown in Fig. 4, built on MATLAB's Simulink, was used to obtain the results that can be seen in Fig. 5
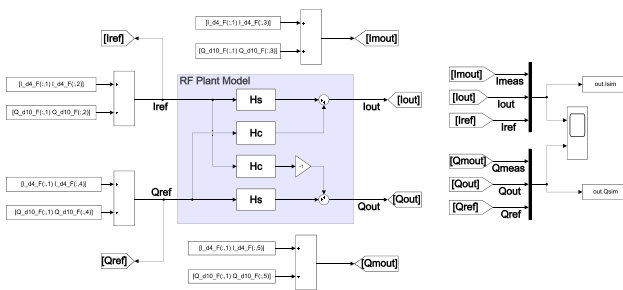
Figure 4: Simulink's block diagram of Sirius RF Plant model.
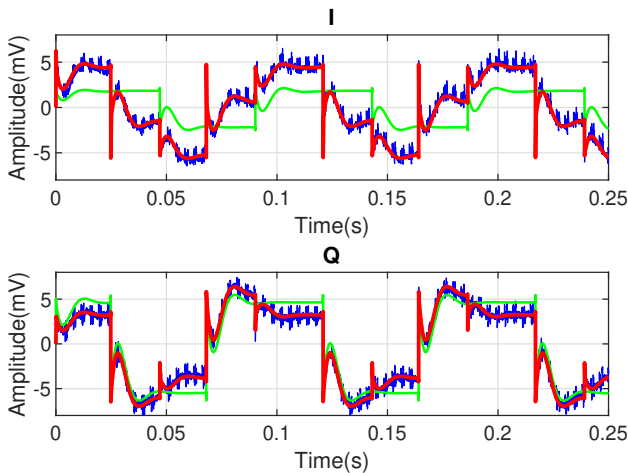
Figure 5: Simulation output (red) when driven by a linear combination of the validation data inputs (green) compared with the same linear combination of the validation data outputs (blue).

CONCLUSION

The estimated models were able to satisfactorily describe the RF plant dynamics around the operating point. Despite the limitations, it can be used to fine tune the LLRF PI loops by making use of MATLAB's Control Toolbox. Further studies should be conducted to refine the models and include beam-loading effects.

ACKNOWLEDGEMENTS

REFERENCES

[1] A. P. B. Lima, D. Daminelli, M. Hoffmann Wallner, F. K. G. Hoshino, I. Carvalho de Almeida, and R. H. A. Farias. Sirius Storage Ring RF System Status Update. Number 13 in International Particle Accelerator Conference. JACoW Publishing, Geneva, Switzerland. presented at IPAC'22, Bangkok, Thailand, Jun. 2022, paper TUPOST014, this conference.

[2] A. Salom, R.H.A. Farias, F.K.G. Hoshino, A.P.B. Lima, and F. Pérez. Sirius Digital LLRF. In *Proc. 10th International Particle Accelerator Conference (IPAC'19), Melbourne, Australia, 19-24 May 2019*, number 10 in International Particle Accelerator Conference, pages 4244–4247, Geneva, Switzerland, Jun. 2019. JACoW Publishing. https://doi.org/10.18429/JACoW-IPAC2019-THPTS060

[3] A. P. B. Lima, F. K. G. Hoshino, C. F. Carneiro, R. H. A. Farias, and A. Salom. *Sirius Digital Low-Level RF Status*. *arXiv preprint arXiv:1910.08499*, 2019.

[4] L. Liu, M.B. Alves, A.C.S. Oliveira, X.R. Resende, and F.H. de Sá. Sirius Commissioning Results and Operation Status. In *Proc. IPAC'21*, number 12 in International Particle Accelerator Conference, pages 13–18. JACoW Publishing, Geneva, Switzerland, 08 2021. https://doi.org/10.18429/JACoW-IPAC2021-MOXA03

[5] Control system toolbox. https://www.mathworks.com/products/control.html.

[6] Nutaq. https://nutaq.com/products/picodigitizer-125-series.

[7] T Schilcher. RF applications in digital signal processing. 2008.

[8] Luis Aguirre. *Introdução à Identificação de Sistemas*. Editora UFMG, 2015.

[9] R Garoby. Low level RF and feedback. page 35 p, Jun 1997.

[10] System identification toolbox. https://www.mathworks.com/products/sysid.html.